

Recent Advances in the Detection of Lead Ions using Nanoparticle-Based Sensors

Himani P. Khawashi ¹, Vilas A. Chavan ² , Devidas S. Bhagat ^{3,*} , Satish U. Deshmukh ⁴

¹ Department of Applied Chemistry, Karunya Institute of Technology and Sciences (Deemed to be University), Karunya Nagar, Coimbatore - 641 114, Tamil Nadu, India; hpkhawashi@gmail.com (H.P.K.);

² Department of Forensic Science, School of Paramedics and Allied Health Science, Centurion University of Technology and Management, Vizianagaram - 535 003, Andhra Pradesh, India; vilas.chavan47@gmail.com (V.A.C.);

³ Department of Forensic Chemistry and Toxicology, Government Institute of Forensic Science, Aurangabad - 431 004, Maharashtra, India; devidas.bhagat@gov.in (D.S.B.);

⁴ Department of Chemistry, Deogiri College, Aurangabad 431005, (M.S), India; satishud@gmail.com (S.U.D.);

* Correspondence: devidas.bhagat@gov.in (D.S.B.);

Scopus Author ID 57201065245

Received: 4.07.2022; Accepted: 15.08.2022; Published: 26.12.2022

Abstract: Even in trace amounts, lead is a pollutant that harms people and wildlife. We thoroughly examined more than a hundred articles on current developments in the detection of lead ions using nanoparticle-based sensors for this work. Lead ions' identification and reduction should be prioritized due to their dangerous nature to stop the severe pollution brought on by heavy metals. It is necessary to have on-site detecting technology to find heavy metal-polluted areas quickly. However, this advanced, commercially viable technology is hard to come by. Nano-based sensors improve spectral methods' sensitivity, selectivity, and detection limits, yet more attenuation is needed in hazardous pollution scenarios. It is concluded that, as research advances and methodological barriers are removed, nanotechnology offers a viable approach to lead detection in aquatic settings as well as forensic samples. These technologies will considerably support continuous environmental monitoring.

Keywords: nanoparticle; environmental; pollutant; toxicity; lead ions; poisoning; nano-sensor.

© 2022 by the authors. This article is an open-access article distributed under the terms and conditions of the Creative Commons Attribution (CC BY) license (<https://creativecommons.org/licenses/by/4.0/>).

1. Introduction

Although fast industrialization has enormous benefits for humanity, it also has certain dangerous side effects, such as the release of wastewater containing heavy metals into the environment, which causes their widespread distribution in the atmosphere. Heavy metals are "Low-density chemical components that are highly toxic" and "metals with atomic weights between 63.5 and 200.6 g mol⁻¹ and a specific gravity greater than 5 g cm⁻³" [13]. Because heavy metals cannot degrade, they are problematic for both humans and the environment. It alters the metabolic life cycle by attaching to the sulphonyl group in proteins. Some heavy metals, such as Zn, Cu, Fe, Co, Mn, and others, are essential to life in small doses, and their toxicity results from exposure above the allowable limit [4-6].

Conventional analytical methods, for example, spectroscopic techniques, can analyze metal particles quantitatively. However, their implementation can be hindered by costly gear and complex techniques [7,8]. Given these drawbacks, current attention is focused on developing sensors for the on-site identification of metallic ions with great sensitivity, rapid response times, and selectivity. Techniques that are more thought to fit the condition include laser-induced breakdown spectroscopy (LIBS) [9], electrochemical [10], and optical [11]

methods. Among them, optical sensors have been given more consideration [12-15]. To develop such systems, two significant viewpoints should be considered: the immobilizing platform (optical, electrochemical) and the receptor (heavy metal ionophore or organic receptor) [16].

Till now, different sensors have been designed using different nanomaterials such as carbon, metallic and magnetic nanomaterials, graphene-based nanomaterials, and quantum dots depending on various optical signal transduction principles [17-22]. The simple design, functionalization, easy and simple detection, and altered properties of bulk materials make nanomaterials applicable for developing optical sensors [23].

Lead (Pb^{+2}) is among the most dangerous heavy metals [24-26]. Small amounts of lead ions are needed for cell signaling and signal transit in human and plant cells [27]. But these ions, if present in abundance, bind with other regulatory proteins in the body despite specific binding sites and cause impaired mechanisms through free radical generation. As a result, DNA damage [28-30], increased lipid peroxidation, and sulfhydryl homeostasis may occur [30,31]. Lead ions show toxicity through inhibiting enzymes, oxidative stress, and reduced antioxidant metabolism. The toxicity processes of lead ions are discussed in this work, along with the nanoparticle sensor technology that has supported the many developments in lead sensing and detection [32-35].

1.1. Toxicity range of lead and its exposure.

In the human body, lead is found bonded with RBCs and gradually eliminated via urine over some time. Lead is present in the skeleton for about 20-30 years after death. Children are more vulnerable to exposure to lead than adults as their blood-brain barrier is not fully developed; the lead can penetrate the blood-brain barrier causing neurodegenerative diseases [36]. Since metals are important for cellular functions, their concentration should not exceed the permissible limit. Otherwise, it will result in toxic effects. The permissible limit of lead is 0.05 mg/L and 0.05 mg/L, according to WHO and BIS, respectively [37,38].

Humans get lead exposure from air and food to generally equivalent extents. Earlier, lead exposure was seen in food prepared in pots that were composed of lead. 10-15% of lead gets into the body of adults through food [39-41]. Mainly, lead discharges to surrounding air have contaminated the environment, with over half of lead outflows from petrol. Lead in the air can eventually accumulate in soil and water, getting exposed to humans by the consumption of food and water [42-45]. Exposure can also occur in mines, smelters, battery plants, and the glass industry.

1.2. Toxicity mechanisms of lead poisoning.

Lead affects a wide range of physiological, biochemical, and behavioral activities in both animals and people [46-48], including the neurological [49], hemopoietic [50], cardiovascular [51], renal [52], hepatic [53], and reproductive systems [54,55]. Yiin and Lin (1995) showed substantial malondialdehyde enhancement when lead was exposed to linolenic, linoleic, and arachidonic acid, which increased lipid peroxidation, causing damage to the cell membranes of animals [56-58]. Again, lead exposure causes lipid peroxidation, and the amount of peroxidation was proportional to the lead levels [59,60].

Lead toxicity's primary targets are changes in the shape of RBCs and inhibition of the heme production pathway. The production process requires the cytosolic sulfhydryl enzyme

alpha-aminolevulinic acid dehydratase. According to reports, blood lead levels of roughly 15 µg / dl are sufficient to stop an enzyme from working [61]. Lead also reduces ferrochelatase activity, which is necessary for the final stage of heme production. Figure 1 illustrates how reduced synthesis of heme results from insufficient normal ALAD activity to convert two ALA molecules into porphobilinogen.

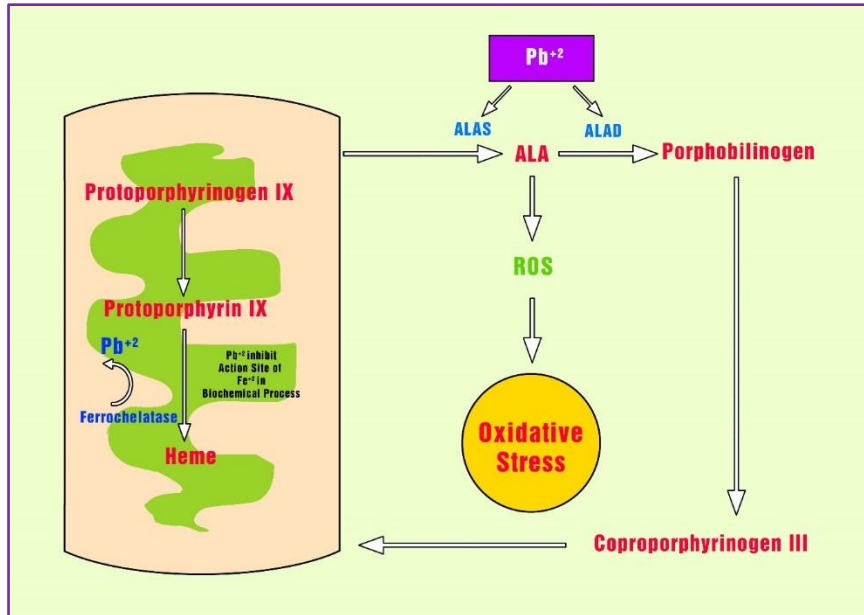


Figure 1. Effect of lead on biochemical process [61].

As lead crosses the blood-brain barrier, it can cause mental and behavioral issues, neuromuscular exhaustion, and even coma [62]. When lead is present, GABA is released and binds to the synaptic membrane [63]. The growing organism has a 5-fold increased lead absorption since it does not have a functioning blood-brain barrier. In both suckling and adult rats, perinatal exposure can affect their neurochemical and behavioral makeup. Additionally, mice exposed to acetate in drinkable water have been shown to develop dysfunctions. Lead increases ROS. Increased intracellular Ca²⁺ and ROS levels reduce mitochondrial capacity and cause the release of cytochrome C, which leads to apoptosis, Figure 2 [64].

According to several research, lead affects the activity of antioxidant molecules like GSH and enzymes like 6-phosphate dehydrogenase (G6PD), glutathione peroxidase (GPx), catalase, and SOD in animals [65-67]. A study on lead-exposed employees revealed a direct correlation between blood lead and MAD levels in RBCs. The inhibition of glutathione reductase and glutathione S-transferase by lead has an impact on the metabolism of glutathione. These enzymes raise levels of ALAD and oxidize hemoglobin [68].

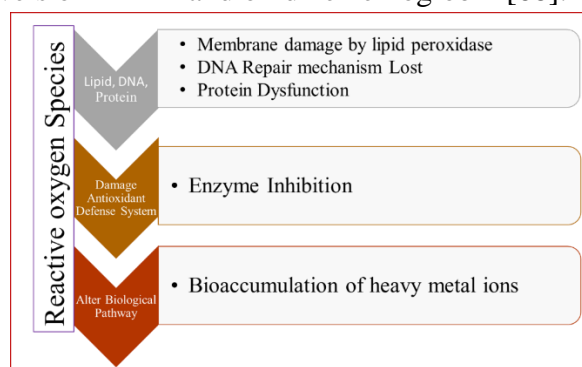


Figure 2. Generation of reactive oxygen species (ROS) due to inhibition of heavy metal ions. Reproduced with permission from Elsevier [69].

2. Detection of Lead Ions using Nanoparticles

For the precise detection of Pb^{2+} , a colorimetric technique based on aptamers was created [69]. On graphene, Fe_3O_4 NPs and AuNPs were produced to create composites of graphene/ Fe_3O_4 -AuNP that acted as a peroxidase mimic for the catalysis of color response. The magnetic amine beads held the Pb^{2+} aptamer in place. In the presence of lead ions, the Pb^{2+} aptamer's complementary strands were adhered to the surface of the nanozyme composite, limiting catalytic performance and the color response, as seen in Figure 3. The relationship between the target lead ionic strength and the solution's color and value A_{652} was inverse. Pb^{2+} was discovered between 1-300 ng/mL with a LOD of 0.63 ng/mL [70]. Xu *et al.* (2020) created the biosensor using a SERS method to detect Pb^{2+} ions. By using specific identification, the Pb^{2+} was found to be a magnetic SERS substratum over $DSFe_3O_4@Au@Ag$ NPs. Wu *et al.* (2019) effectively recognized and reasonably expected Pb^{2+} ion with an "inner rule" and a detection range of 1.79 pg mL^{-1} utilizing DNA enzyme efficiency and the quenching effects of Gold NP [71,72].

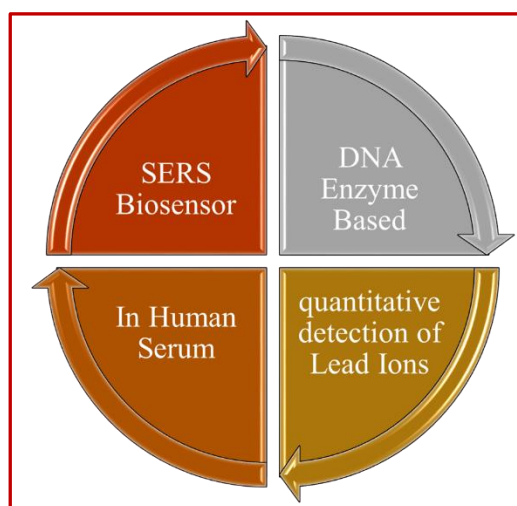


Figure 3. Detection of Pb^{2+} ions in colorimetric assay [70].

The specific and sensitive detection of Pb^{2+} was carried out with $Au@p-rGO$ nanoparticles using the complementary base pairing principle [73]. Due to the selectivity, the sensor could detect Pb^{2+} specifically even when other interfering ions are present [74]. Wang *et al.* (2020) documented the construction of a highly sensitive Pb^{2+} sensor based on the FRET mechanism between upconversion nanoparticles (UCNPs) and Au NPs. With the hybridization of two complementary DNA strands, the FRET assay was developed for quenching the green fluorescence of upconversion nanoparticles. The binding between UCNP aptamers and Pb^{2+} resulted in the formation of G-quadruplexes, resulting in unwound DNA for fluorescence recovery, specifically detecting Pb^{2+} , as shown in Figure 4 [75]. Chen *et al.* (2020) created a luminous Pb^{2+} nanoprobe using the same fluorescence mechanism. Both magnetic Fe_3O_4 nanoparticles with gold modifications and aptamer-functional upconversion nanoparticles (UCNPs) were created. In the absence of lead, the UCNPs and MNPs-GNPs fluoresced at 547 nm, but in the presence of lead, the dsDNA between the UCNPs and MNPs-GNPs is broken, and the fluorescence is recovered. With a linear range of 25-1400 nM and a LOD of 5.7 nM, this effect enables the measurement of Pb^{2+} [76].

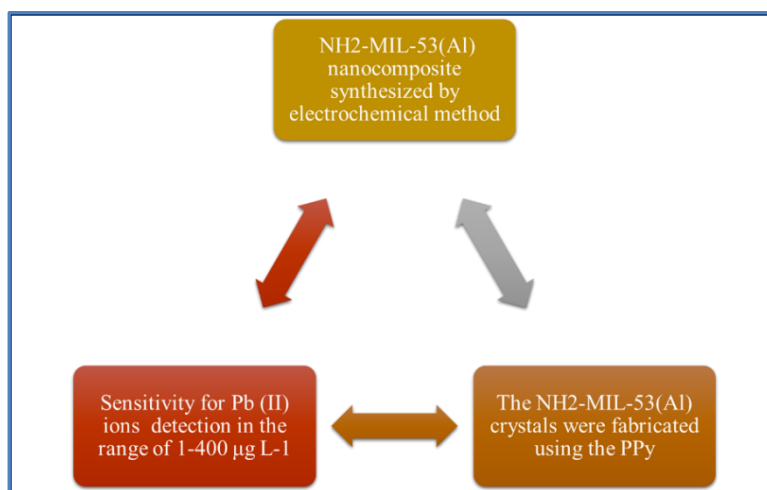


Figure 4. Fluorescence sensing assay constructed for Pb²⁺ ions detection. Reproduced with permission from Elsevier [75].

Pb²⁺ ions were visually identified with a LOD of 55 pM in 100 µl (reaction concentration) and 1,108 nM in 5 µl (sample concentration) by combining nanoparticles-amplified magnetophoresis with Mie scattering [77]. A novel fluorescent compound based on coumarin was created by Khan *et al.* in 2020, and it was then described (with solvatochromic properties). Its local environment-sensitive property enhanced lead detection with the AuNPs (AuNPs/1 conjugate) combination. The color shift in the visual region from light brown to green and spectral changes in UV-Vis was observed (as shown in Figure 5 and Figure 6) [78].

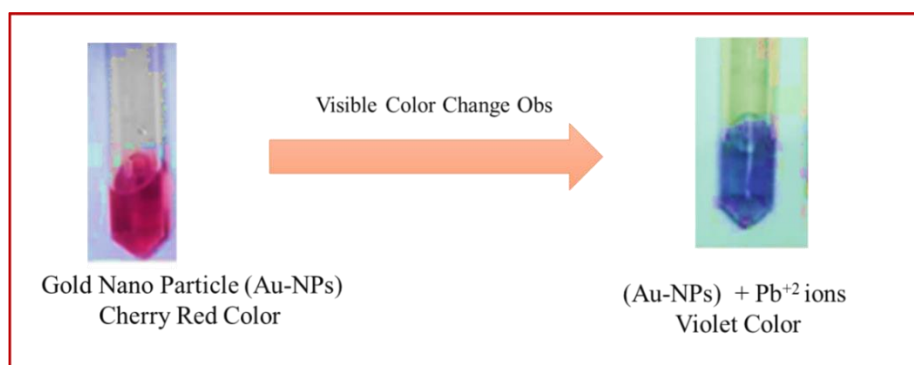


Figure 5. Addition of the Pb²⁺ ions in the solution of gold nanoparticles, the color changed from red to violet. Reproduced with permission from Elsevier [78].

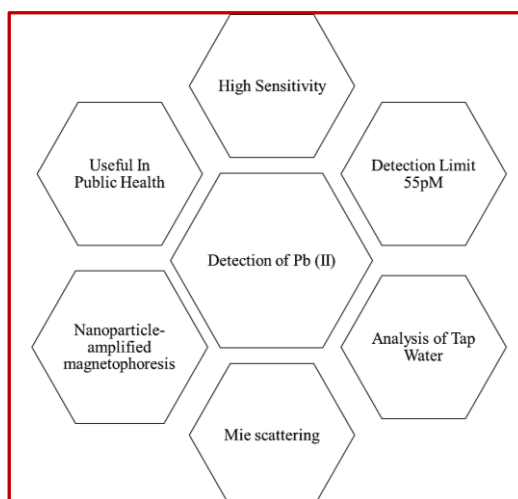


Figure 6. The change in Colour is accompanied by Florescence Enhancement. Reproduced with permission from Elsevier [78].

Qin *et al.* (2020) are stated to be using a sensitive electrochemical sensing platform based on AuNPs-CD-GS nanocomposite for individual/simultaneous determination of Cd^{2+} and Pb^{2+} with a broad linear detection range ($40 - 1200 \text{ g L}^{-1}$) and low LOD [79]. The dispersed AuNPs-CD-GS is manufactured using a simple one-pot synthesis using hydrazine and some-CD as reducing agents for reducing GO and gold ions and optimizing HAuCl_4 concentration. Due to the fast adsorption absorption of Cd^{2+} and Pb^{2+} on any CD, the nanocomposite demonstrates high capture capability. Azimi *et al.* (2020) used citrate-capped Ag nanoparticles to evaluate Pb^{2+} based on an aggregation of silver nanoparticles. In the presence of Pb^{2+} , the solution color changed from light yellow to violet depending on Pb^{2+} concentration. Depending on the lead concentration, the aggregation caused the local surface plasmon resonance region to shift from 580 nm to 440 nm. In Figure 7 [80], the LOD of 0.056 mol L^{-1} was discovered.

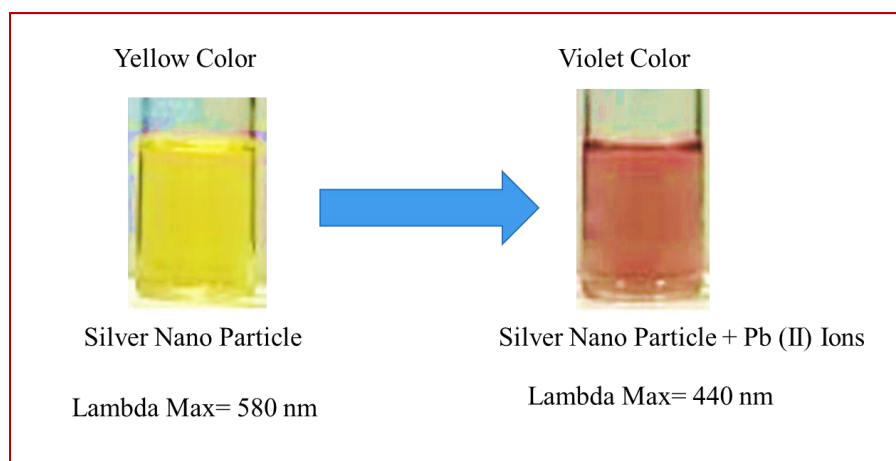


Figure 7. Detetction of Pb^{2+} using silver nanoparticle. Reproduced with permission from Elsevier [80].

Yin *et al.* (2020) prepared nano-Au electrodes that were manufactured to detect Pb^{2+} sensitively and demonstrated a highly selective response to Pb^{2+} . The Pb^{2+} electrochemical detection was performed by differential pulse stripping voltammetry (DPSV) [81]. Ahmadian-Fard-Fini *et al.* (2020) manufactured photoluminescence (PL) nano-fibers based on electrospinning mechanisms for the detection of Hg^{2+} and Pb^{2+} ions [82]. Square wave anodic voltammetry stripping was used by Dutta *et al.* (2019) and Maleki *et al.* (2019) to create metal nanoparticles for lead (Pb^{2+}) detection. Gold nanoparticles were used by Silva-De Hoyos *et al.* (2020) to detect lead ions using plasmonic and fluorescence techniques [83]. The brain's neuromelanin (NM) can transform environmental poisons into stable compounds and inhibit their ability to harm. Zhang *et al.* (2020) created a dopamine and amino acid that mimicked NM. Figure 8 [84] shows that the NM exhibited intense fluorescence, which Pb^{2+} can quench.

Square wave stripping voltammetry (SWSV) variables were independently tuned in the study by Dutta *et al.* (2018) to identify As^{+3} , Hg^{2+} , and Pb^{2+} , and peak heights, I_p , was achieved for a variety of NP loadings. For each analyte and particle shape, the I_p values showed a distinct trend that varied about NP loading. With the same loading of As (III), AuNSs exhibited larger peak heights than AuNPs. High AuNP loadings resulted in a significant reduction in I_p values for Hg^{2+} , but high AuNS loadings resulted in a little reduction. The I_p values linked to Pb were not significantly impacted by NP loadings $^{2+}$. These results imply that the loading and form of gold nanostructures can affect the effectiveness of electrochemical heavy metal identification and should be considered [85].

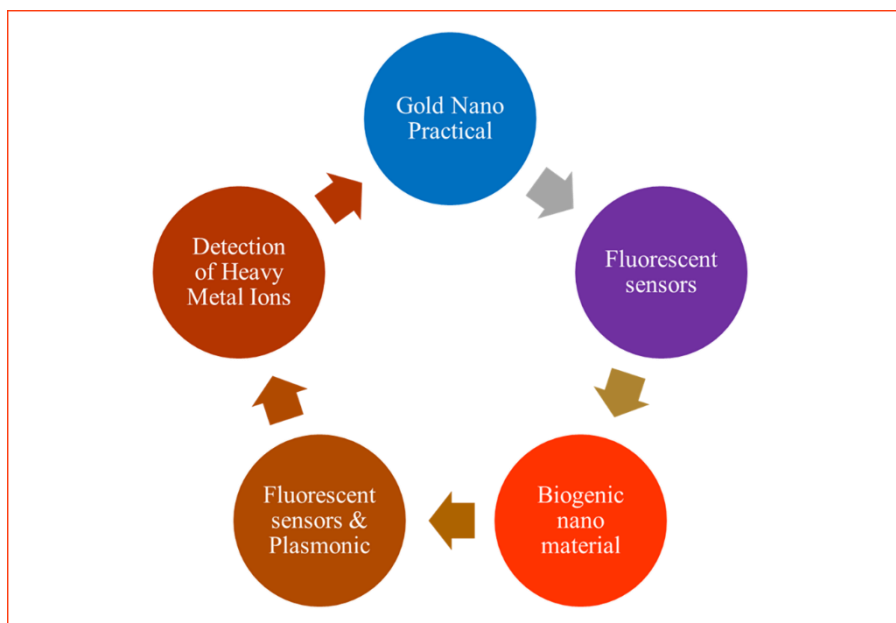


Figure 8. Biogenic Au NPs used for the detection of heavy metal ions. Reproduced with permission from ScienceDirect [84].

A glassy carbon electrode (GCE) has been developed in the study by Xu *et al.* (2019) using PPy NPs, polydopamine, CQAS, and LSN as PPy dispersants. With a detection limit of 55 nM, the modified GCE demonstrated remarkable sensitivity and selectivity for Pb^{2+} in the concentration range of 0.1 to 50 M. Hg^{2+} and Cu had no effect on the sensor, and the redox potential for Pb^{2+} was approximately 0.55 V. According to the results of the time-dependent stability test, this sensor can sustain good reproducibility for a month. Utilizing this sensor, Pb^{2+} in wastewater samples was determined [86]. In the study by Zhang *et al.* (2019), the Pd@PAC modified glassy carbon electrode (Pd@PAC/GCE) was employed for the square wave anodic stripping voltammetry detection of trace Cd^{2+} , Pb^{2+} , and Cu^{2+} ions (SWASV). Under the same experimental conditions, it demonstrated excellent anti-interference, sensitive and selective identification of heavy metals concurrently and individually, as well as repeatability, reproducibility, and stability [87].

In contrast to other metal ions, NDTM-AuNPs demonstrated a sensitive and selective spectrophotometric signal with Pb^{2+} in the study by Sengan *et al.* (2020). A linear response was seen in the range of 0 to 30 M for the colorimetric changes resulting from Pb^{2+} concentration ($R^2 = 0.9942$). The detection limit by unaided sight was determined to be 10 M and by spectrophotometry to be 0.35 M. The Pb^{2+} ions in tap water and wastewater may be determined with success using the suggested method [88]. The optimal desorption conditions were achieved using 500 L of 0.5 mol L^{-1} HNO_3 as the eluant in the Silva *et al.* (2019) study. The relative standard deviation (RSD) and limit of quantification (LOQ) were 16.48 g L^{-1} and 0.25 percent, respectively. It was discovered that the linear range was 16.48-500 g L^{-1} . Recovery tests on samples of mineral water, micellar water, and aqueous makeup remover were used to gauge the accuracy; the results ranged from 95.94 to 118 percent [89].

The limit of detection and linear range for the "on-off" approach of MW G-BSA-AuNCs for Pb^{2+} ion identification were 0.28 and 1-20 nM, respectively, in the study by Ryavanaki *et al.* (2020). The MW G-BSA-AuNCs probe's recoveries, which were utilized to find the presence of the Pb^{2+} ion in tap water, ranged from 93.8 to 102.2 percent, with an average of 97.1 percent. In comparison to the often utilized "turn-o" methods of MW BSA-AuNCs, the "off-on" method can offer a lower detection limit, improved selectivity, and better

recovery [90]. The linear range for Pb²⁺ determination in the study by Sahu *et al.* (2020) is 10–100 ng mL⁻¹, with limits of quantitative determination of 5.28 and 17.62 ng mL⁻¹, correspondingly. The accurate recovery rate of 95.8 to 96.6 percent demonstrated the method's selectivity for Pb²⁺ measurement from complicated sample matrices. The benefits of the suggested approach for determining Pb²⁺ in samples of onions include its simplicity, selectivity, and reproducibility [91].

The detection limit of HP-CD-AuQDs (32 nm) was less in the study of Kou *et al.* (2020). The HP-CD-AuQDs (25 nm) displayed the greatest Pb²⁺ selectivity. After 32-nm S-CD-AuQDs were functionalized, aggregation took place. A solution Pb²⁺ concentration of 83.3 mol/L corresponds to all of the ocular detection limits. Although the 25-nm HP-CD-AuQDs had a lower detection limit, their selectivity was poor. Additionally, 25-nm S-CD-AuQDs exhibit greater Pb²⁺ colorimetric selectivity. Pb²⁺ in tap water may be detected colorimetrically with excellent reproducibility [92]. The MOF was utilized as a sensitive probe in the study by Venkateswarlu *et al.* (2020) for the quick and ultrasensitive identification of Pb²⁺ ions at a concentration of 7.7 pM, one of the lower detection limits recorded for such a system. The MOF exhibits strong selectivity for different transition metal ions, which can be competitively coupled to the ligand [93].

Table 1 depicts the comparative summary of the detection sensitivity achieved by different nanoparticles and various lead interfaces.

Table 1. Summary of the detection sensitivity achieved by different nanoparticles and various interfaces of lead ions.

Sr. No.	Nanoparticle Fabricated	Functionalizing agent	Method of detection	Liner Range	Limit of Detection	Sensitivity	Reference
1	Graphene/Fe ₃ O ₄ -AuNPs	Aptasensor	Colorimetric Detection	1–300 ng/mL	0.63 ng/mL	-	[70]
2	Fe ₃ O ₄ @Au@Ag NP	DNAzyme	(SERS)	0.01 to 1.0 nM	5 pM	-	[71]
3	Gold Nps and CdSe/ZnS quantum dots	DNA Substrate	Fluorescence	10 to 100 ng mL ⁻¹	1.79 pg mL ⁻¹	-	[72]
4	Gold modified graphene nanocomposite	Aptasensor	Electrochemical Detection	5 pmol/L to 1 μmol/L	1.67 pmol/L	-	[72]
5	Magnetite (Fe ₃ O ₄) nanoparticles	-	ICP-MS	0.028–30.0 μM	0.0084 μM	-	[72]
6	Polypyrrole nanocomposite	-	Electrochemical Detection	1–400 μg L ⁻¹	0.315 μg L ⁻¹	-	[74]
7	Fe ₃ O ₄ @PDA@MnO ₂ core-shell nanocomposites	-	Electrochemical Detection	0.1–150 μg L ⁻¹	0.03 μg L ⁻¹	-	[75]
8	Gold Nps	Aptamer	Fluorescence resonance energy transfer (FRET)	0 to 50 nM	4.1 nM	-	[75]
9	Magnetite-modified gold nanoparticles	Aptamer	FRET	25–1400 nM	5.7 nM	-	[76]
10	Gold Nanoparticle	-	Mie scattering	-	55 pM in 100 μl reaction concentration	-	[77]
11	Gold Nps	Coumarin derivative	Fluorescence	-	-	-	[78]

Sr. No.	Nanoparticle Fabricated	Functionalizing agent	Method of detection	Linear Range	Limit of Detection	Sensitivity	Reference
12	Gold Nps	β -cyclodextrin-graphene	Electrochemical Detection	40 - 1200 $\mu\text{g L}^{-1}$	-	-	[79]
13	Silver Nps	deferoxamine	Local surface plasmon resonance (LSPR)	0.19 to 1.29 $\mu\text{mol L}^{-1}$	0.056 $\mu\text{mol L}^{-1}$	-	[80]
14	Gold Nanoparticles	-	Differential pulse stripping voltammetry (DPSV)	0.5 to 10 M	0.06 M	0.27996 mA M^{-1}	[81]
15	Cellulose acetate nano-fibers	-	Photoluminescence	-	-	-	[82]
16	Gold nanoparticles	-	Fluorescence	-	-	-	[83]
17	Neuromelanin nanoparticles	-	-	10-50 mg L^{-1}	2 mg L^{-1}	-	[84]
18	Iron oxide nanoparticles	Polyamidoamine dendrimer	SWASV	0.5 to 80 ng mL^{-1}	0.17 ng mL^{-1}	-	[85]
19	Antimony nanoparticles	-	Electrochemical Detection	0.1 to 3.0 $\mu\text{mol L}^{-1}$	2.01 nmol L^{-1}	-	[86]
20	Gold nanoparticles	N-decanoyltromethamine	Colorimetric detection	0-30 μM	10 μM	-	[87]
21	Gold Nanoclusters	-	-	1-20 nM	0.28nM	-	[88]
22	Au/Ag Bimetallic Nanoparticles	-	-	10-100 ng mL^{-1}	5.28m/L	-	[89]
23	Nanocrystalline Gold	β -cyclodextrin	Colorimetric Detection	-	83.3 $\mu\text{mol/L}$	-	[90]
24	Metal-Organic Framework Nanoparticles	-	Reversible Fluorescence Switching	-	7.7 pM	-	[91]
25	Ag@Pt core-shell NPs	-	Square wave anodic stripping voltammetry	-	0.8 nM	-	[92]
26	Gold nanoparticle-graphene-selenocysteine composite	-	Square wave anodic stripping voltammetry	-	0.05 ppb	-	[93]

3. Discussion

The current study examines lead ions, their pollution sources, and their toxicity mechanism in addition to nanoparticle-based detection methods. Due to the harmful nature of lead ions, their identification and elimination should be given priority to stop the severe pollution caused by heavy metals. Currently, on-site detection equipment that can quickly locate heavy metal-polluted locations is required. But it's hard to find this developed, marketable technology.

Nano-based sensors boost the sensitivity, selectivity, and limit of detection of spectral approaches, although greater attenuation is required in hazardous pollution situations. To build on-site detection, it is crucial to consider matrix interference and critical analyte analysis. At first, as environmental contamination rises, cutting down on the analysis time is crucial. The

enhanced sensitivity mechanics that can be achieved by fusing spectral approaches with theoretical calculations also need to be demonstrated through actual testing. Overall, we realized that nanotechnology provides a promising alternative to lead identification in aqueous environments and forensic evidence. These technologies will significantly contribute to the ongoing environmental monitoring as researchers go forward and remove the method's obstacles.

4. Conclusions

The present study analyses the lead ions and their origins of contamination and toxicity mechanism along with nanoparticle-based detection technologies. Due to lead ions' toxic effects, their detection and reduction should be prioritized to prevent heavy metal-related pollution from becoming severe. On-site detection kits, able to track heavy metal polluted sites easily, are a current necessity. But this form of mature and commercialized technology is scarce. The sensitivity, selectivity, and detection limits of spectral methods are increased with the nano-based sensors, but more attenuation is needed in the critical pollution situation. The matrix interference and critical analysis of the analyte are very much required to develop on-site detection. Firstly, decreasing the analytical time is important as environmental pollution is increasing. In addition, direct experiments need evidence to reveal the enhanced sensitivity mechanisms that can be accomplished by combining spectral techniques with theoretical calculations.

We concluded that nanotechnology offers a promising approach to lead detection in aquatic settings and forensic samples. These methods will significantly contribute to the day-to-day monitoring of the environment as researchers move forward and break down the bottlenecks of these methods.

Funding

This study received no external funding.

Acknowledgments

The contributors to this work, whether direct or indirect, have our sincere gratitude.

Conflicts of Interest

The authors declare no conflict of interest.

References

1. Järup, L. Hazards of heavy metal contamination. *Br. Med. Bull.* **2003**, *68*, 167-182, <https://doi.org/10.1093/bmb/ldg032>.
2. Tekaya, N.; Saiapina, O.; Ben Ouada, H.; Lagarde, F.; Ben Ouada, H.; & Jaffrezic-Renault, N. Ultra-sensitive conductometric detection of heavy metals based on inhibition of alkaline phosphatase activity from *Arthrospira platensis*. *Bioelectrochemistry*, **2013**, *90*, 24-29, <https://doi.org/10.1016/j.bioelechem.2012.10.001>
3. Turdean, G. Design and Development of Biosensors for the Detection of Heavy Metal Toxicity. *Int. J. Electrochem. Sci.* **2011**, 1-15, <https://doi.org/10.4061/2011/343125>
4. Kumar, P.; Kim, K.; Bansal, V.; Lazarides, T.; & Kumar, N. Progress in the sensing techniques for heavy metal ions using nanomaterials. *J Ind Eng Chem.* **2017**, *54*, 30-43, <https://doi.org/10.1016/j.jiec.2017.06.010>.

5. Bagal-Kestwal, D.; Karve, M.; Kakade, B.; & Pillai, V. Invertase inhibition based electrochemical sensor for the detection of heavy metal ions in aqueous system: Application of ultra-microelectrode to enhance sucrose biosensor's sensitivity. *Biosens. Bioelectron.* **2008**, *24*, 657-664, <https://doi.org/10.1016/j.bios.2008.06.027>.
6. Tag, K.; Riedel, K.; Bauer, H.; Hanke, G.; Baronian, K.; & Kunze, G. Amperometric detection of Cu²⁺ by yeast biosensors using flow injection analysis (FIA). *Sens. Actuators B Chem.* **2007**, *122*, 403-409, <https://doi.org/10.1016/j.snb.2006.06.007>.
7. Zhou, Y.; Tang, L.; Zeng, G.; Zhang, C.; Zhang, Y. and Xie, X. Current progress in biosensors for heavy metal ions based on DNAzymes/DNA molecules functionalized nanostructures: A review. *Sens. Actuators B Chem.* **2016**, *223*, 280-294, <http://dx.doi.org/10.1016/j.snb.2015.09.090>.
8. Pandey, S.; Singh, P.; Singh, J.; Sachan, S.; Srivastava, S. and Singh, S. Nanocarbon-based Electrochemical Detection of Heavy Metals. *Electroanalysis* **2016**, *28*, 2472-2488, <https://doi.org/10.1002/elan.201600173>
9. Meng, D.; Zhao, N.; Wang, Y.; Ma, M.; Fang, L.; Gu, Y.; Jia, Y. and Liu, J. On-line/on-site analysis of heavy metals in water and soils by laser induced breakdown spectroscopy. *Spectrochim. Acta B: At. Spectrosc* **2017**, *137*, 39-45, <https://doi.org/10.1016/j.sab.2017.09.011>.
10. Lee, Y.; Han, J.; Kwon, S.; Kang, S. and Jang, A. Development of a rotary disc voltammetric sensor system for semi-continuous and on-site measurements of Pb²⁺. *Chemosphere* **2016**, *143*, 78-84, <http://dx.doi.org/10.1016/j.chemosphere.2015.05.069>.
11. Guo, J.; Zhou, M. and Yang, C. Fluorescent hydrogel waveguide for on-site detection of heavy metal ions. *Sci. Rep.* **2017**, *7*, <https://doi.org/10.1038/s41598-017-08353-8>.
12. Choi, S.; Persano, L.; Camposeo, A.; Jang, J.; Koo, W.; Kim, S.; Cho, H.; Kim, I. and Pisignano, D. Electrospun Nanostructures for High Performance Chemiresistive and Optical Sensors. *Macromol. Mater. Eng.* **2017**, *302*, 1600569, <https://doi.org/10.1002/mame.201600569>.
13. Zhang, N.; Qiao, R.; Su, J.; Yan, J.; Xie, Z.; Qiao, Y.; Wang, X. and Zhong, J. Recent Advances of Electrospun Nanofibrous Membranes in the Development of Chemosensors for Heavy Metal Detection. *Small* **2017**, *13*, 1604293, <https://doi.org/10.1002/smll.201604293>.
14. Schoolaert, E.; Hoogenboom, R.; De Clerck, K. Colorimetric Nanofibers as Optical Sensors. *Adv. Funct. Mater.* **2017**, <https://doi.org/10.1002/adfm.201702646>.
15. Piriya V.S. A.; Joseph, P.; Daniel S.C.G. K.; Lakshmanan, S.; Kinoshita, T. and Muthusamy, S. Colorimetric sensors for rapid detection of various analytes. *Mater. Sci. Eng. C* **2017**, *78*, 1231-1245, <https://doi.org/10.1016/j.msec.2017.05.018>.
16. Liu, Y.; Deng, Y.; Dong, H.; Liu, K.; & He, N. Progress on sensors based on nanomaterials for rapid detection of heavy metal ions. *Sci China Chem* **2016**, *60*, 329-337, <https://doi.org/10.1007/s11426-016-0253-2>.
17. Terra, I.A.A.; Mercante, L.A.; Andre, R.S.; Correa, D.S. Fluorescent and Colorimetric Electrospun Nanofibers for Heavy-Metal Sensing. *Biosensors* **2017**, *7*, 61, <https://doi.org/10.3390/bios7040061>.
18. Salek Maghsoudi, A.; Hassani, S.; Mirnia, K.; Abdollahi, M. Recent Advances in Nanotechnology-Based Biosensors Development for Detection of Arsenic, Lead, Mercury, and Cadmium. *Int J Nanomedicine.* **2021** *16*, 803-832, <https://doi.org/10.2147/IJN.S294417>.
19. Singh, H.; Bamrah, A.; Bhardwaj, S. K.; Deep, A.; Khatri, M.; Brown, R. J. C.; Kim, K.-H. Recent advances in the application of noble metal nanoparticles in colorimetric sensors for lead ions. *Environ. Sci. Nano* **2021**, *8*, 863-889, <https://doi.org/doi:10.1039/d0en00963f>.
20. Cao, J.-T.; Liao, X.-J.; Wang, Y.-L.; Liu, Y.-M. A Novel Photoelectrochemical Strategy for Lead Ion Detection Based on CdSe Quantum Dots Co-Sensitized ZnO-CdS Nanostructure. *J. Electroanal. Chem.* **2021**, *880*, 114828, <https://doi.org/10.1016/j.jelechem.2020.114828>.
21. Adegoke, O.; Daeid, N.N. Alloyed AuFeZnSe Quantum Dots@gold Nanorod Nanocomposite as an Ultrasensitive and Selective Plasmon-Amplified Fluorescence OFF-ON Aptasensor for Arsenic (III). *J. Photochem. Photobiol. A Chem.* **2022**, *426*, 113755, <https://doi.org/10.1016/j.jphotochem.2021.113755>.
22. Pavadai, R.; Amalraj, A.; Subramanian, S.; Perumal, P. High Catalytic Activity of Fluorophore-Labeled Y-Shaped DNAzyme/3D MOF-MoS 2 NBs as a Versatile Biosensing Platform for the Simultaneous Detection of Hg²⁺, Ni²⁺, and Ag⁺ Ions. *ACS Appl. Mater. Interfaces* **2021**, *13*, 31710-31724, <https://doi.org/10.1021/acsami.1c07086>.
23. Yantasee, W.; Lin, Y.; Hongsirakarn, K.; Fryxell, G.; Addleman, R. and Timchalk, C. Electrochemical Sensors for the Detection of Lead and Other Toxic Heavy Metals: The Next Generation of Personal Exposure Biomonitoring. *Environ. Health Perspect.* **2007**, *115*, 1683-1690. <https://doi.org/10.1289/ehp.10190>.

24. Flora, S.; Mittal, M.; & Mehta, A. Heavy metal induced oxidative stress & its possible reversal by chelation therapy. *Indian J Med* **2008**, 501-523. Retrieved 21 August 2020, From <https://pubmed.ncbi.nlm.nih.gov/19106443/>.
25. Flora, S. Structural Chemical and Biological Aspects of Antioxidants for Strategies Against Metal and Metalloid Exposure. *Oxid. Med. Cell. Longev.* **2009**, 2, 191-206, <https://doi.org/10.4161/oxim.2.4.9112>.
26. Tekis, J. Wang. Simultaneous electrochemical detection of multiple heavy metal ions in water, Available online: <https://www.ctc-n.org/products/simultaneous-electrochemical-detection-multiple-heavy-metal-ions-water> **1996**, 1, <https://doi.org/10.1149/1945-7111/ac40c7>.
27. Valko, M.; Morris, H.; & Cronin, M.; Metals, Toxicity and Oxidative Stress. *Curr. Med. Chem.* **2005**, 12, 1161-1208, <https://doi.org/10.2174/0929867053764635>.
28. Labuda, J.; K. Bubnicova, K.; Kovalova, L.; Vanickova, M.; Mattusch, J.; & Wennrich, R. Voltammetric Detection of Damage to DNA by Arsenic Compounds at a DNA Biosensor. *Sensors* **2005**, 5, 411-423, <https://doi.org/10.3390/s5060411>.
29. LI, D.; MORIMOTO, K.; TAKESHITA, T.; & LU, Y. Arsenic Induces DNA Damage via Reactive Oxygen Species in Human Cells. *Environ. Health Prev. Med.* **2001**, 6, 27-32, <https://doi.org/10.1265/ehpm.2001.27>.
30. M. Kessel; S.X.; Liu, A.; Xu, R.; Santella, T.K. Hei. Arsenic induces oxidative DNA damage in mammalian cells, *Mol. Cell. Biochem.* **2002**, 234-235, 301-308, https://doi.org/10.1007/978-1-4615-1087-1_34.
31. Ercal, N.; Gurer-Orhan, H.; Aykin-Burns, N. Toxic metals and oxidative stress part I: mechanisms involved in metal-induced oxidative damage. *Curr Top Med Chem.* **2001**, 1, 529-39, <https://doi.org/10.2174/1568026013394831>.
32. Shan-Yong Chen; Zhi Li; Kun Li; Xiao-Qi Yu. Small molecular fluorescent probes for the detection of lead, cadmium and mercury ions. *Coord. Chem. Rev.* **2021**, 429, 213691, <https://doi.org/10.1016/j.ccr.2020.213691>.
33. Wang, F.; Wang, K.; Kong, Q.; Wang, J.; Xi, D.; Gu, B.; Chen, X. Recent studies focusing on the development of fluorescence probes for zinc ion. *Coord. Chem. Rev.* **2021**, 213636, <https://doi.org/10.1016/j.ccr.2020.213636>
34. Liu, W.; Chen, J.; Xu, Z.; Fluorescent probes for biothiols based on metal complex. *Coord. Chem. Rev.* **2021**, 429, 213638, <https://doi.org/10.1016/j.ccr.2020.213638>.
35. Chen, Z.; Xie, M.; Zhao, F.; Han, S. Application of Nanomaterial Modified Aptamer-Based Electrochemical Sensor in Detection of Heavy Metal Ions. *Foods* **2022**, 11, 1404, <https://doi.org/10.3390/foods11101404>.
36. L, P. (2020). Lead toxicity part II: the role of free radical damage and the use of antioxidants in the pathology and treatment of lead toxicity. *PubMed.* **2020**, 11, 114-127, <https://www.ncbi.nlm.nih.gov/pubmed/16813461>.
37. Valko, M.; Rhodes, C.; Moncol, J.; Izakovic, M.; & Mazur, M. Free radicals, metals and antioxidants in oxidative stress-induced cancer. *Chem.-Biol. Interact.* **2006**, 160, 1-40, <https://doi.org/10.1016/j.cbi.2005.12.009>.
38. Wang, Y.; Wei, Y.; Zhang, H.; Shi, Y.; Li, Y.; & Li, R. Arsenic trioxide induces apoptosis of p53 null osteosarcoma MG63 cells through the inhibition of catalase. *Med. Oncol.* **2011**, 29, 1328-1334, <https://doi.org/10.1007/s12032-011-9848-5>.
39. Wani, A.; Ara, A.; & Usmani, J.; Lead toxicity: a review. *Interdiscip. Toxicol.* **2015**, 8, 55-64, <https://doi.org/10.1515/intox-2015-0009>.
40. Ouyang, Q.; Wang, L.; Ahmad, W.; Rong, Y.; Li, H.; Hu, Y.; Chen, Q. A Highly Sensitive Detection of Carbendazim Pesticide in Food Based on the Upconversion-MnO₂ Luminescent Resonance Energy Transfer Biosensor. *Food Chem* **2021**, 349, 129157, <https://doi.org/10.1016/j.foodchem.2021.129157>.
41. Yuan, M.; Qian, S.; Cao, H.; Yu, J.; Ye, T.; Wu, X.; Chen, L.; Xu, F. An Ultra-Sensitive Electrochemical Aptasensor for Simultaneous Quantitative Detection of Pb²⁺ and Cd²⁺ in Fruit and Vegetable. *Food Chem* **2022**, 382, 132173, <https://doi.org/10.1016/j.foodchem.2022.132173>.
42. Karaouzas, I.; Kapetanaki, N.; Mentzafou, A.; Kanellopoulos, T.D.; Skoulikidis, N. Heavy Metal Contamination Status in Greek Surface Waters: A Review with Application and Evaluation of Pollution Indices. *Chemosphere* **2021**, 263, 128192, <https://doi.org/10.1016/j.chemosphere.2020.128192>.
43. Saravanan, A.; Senthil Kumar, P.; Jeevanantham, S.; Karishma, S.; Tajsabreen, B.; Yaashikaa, P.R.; Reshma, B. Effective Water/Wastewater Treatment Methodologies for Toxic Pollutants Removal: Processes and Applications towards Sustainable Development. *Chemosphere* **2021**, 280, 130595, <https://doi.org/10.1016/j.chemosphere.2021.130595>.

44. Rabai, S.; Teniou, A.; Catanante, G.; Benounis, M.; Marty, J.-L.; Rhouati, A. Fabrication of AuNPs/MWCNTs/Chitosan Nanocomposite for the Electrochemical Aptasensing of Cadmium in Water. *Sensors* **2021**, *22*, 105, <https://doi.org/10.3390/s22010105>.
45. Li, L.; Chen, B.; Luo, L.; Liu, X.; Bi, X.; You, T. Sensitive and Selective Detection of Hg²⁺ in Tap and Canal Water via Self-Enhanced ECL Aptasensor Based on NH₂-Ru@SiO₂-NGQDs. *Talanta* **2021**, *222*, 121579, <https://doi.org/10.1016/j.talanta.2020.121579>.
46. Flora, S.; Flora, G.; & Saxena, G. Environmental occurrence, health effects and management of lead poisoning. *Lead* **2006**, 158-228, <https://doi.org/10.1016/b978-044452945-9/50004-x>.
47. Liu, Jie; and Robert A.; Goyer. "Chapter 23. Toxic Effects of Metals." Casarett & Doull's Essentials of Toxicology, 2e⁻¹ Eds. Curtis D. Klaassen, and John B. Watkins, III. McGraw Hill **2010**, <https://accesspharmacy.mhmedical.com/content.aspx?bookid=449§ionid=3991079>.
48. Ruff, H.; Markowitz, M.; Bijur, P.; & Rosen, J. Relationships among blood lead levels, iron deficiency, and cognitive development in two-year-old children. *Environ. Health Perspect.* **1996**, *104*, 180-185, <https://doi.org/10.1289/ehp.96104180>.
49. Bressler, J.; Kim, K.; Chakraborti, T.; & Goldstein, G. Molecular mechanisms of lead neurotoxicity. *Neurochem. Res.* **1999**, *24*, 595-600, <https://doi.org/10.1023/a:1022596115897>.
50. Lanphear, B. Cognitive Deficits Associated with Blood Lead Concentrations <10 microg/dL in US Children and Adolescents. *Public Health Rep.* **2000**, *115*, 521-529, <https://doi.org/10.1093/phr/115.6.521>.
51. Khalil-Manesh, F.; Gonick, H.; Weiler, E.; Prins, B.; Weber, M.; & Purdy, R. Lead-Induced Hypertension: Possible Role of Endothelial Factors. *Am. J. Hypertens.* **1993**, *6*, 723-729, <https://doi.org/10.1093/ajh/6.9.723>.
52. Damek-Poprawa, M.; & Sawicka-Kapusta, K. Histopathological changes in the liver, kidneys, and testes of bank voles environmentally exposed to heavy metal emissions from the steelworks and zinc smelter in Poland. *Environmental Research* **2004**, *96*, 72-78, <https://doi.org/10.1016/j.envres.2004.02.003>.
53. Sharma, R.P.; Street, J.C. Public health aspects of toxic heavy metals in animal feeds. *J. Am. Vet. Med. Assoc.* **1980**, *177*, 149-153, <https://pubmed.ncbi.nlm.nih.gov/7429947/>.
54. Lancranjan, I.; Popescu, H.; Gavanescu, O.; Klepsch, I.; & Serbănescu, M. Reproductive Ability of Workmen Occupationally Exposed to Lead. *Arch. Environ. Health* **1975**, *30*, 396-401, <https://doi.org/10.1080/00039896.1975.10666733>.
55. Martin J. J.; Ronis Thomas, M Badger. Endocrine mechanisms underlying the growth effects of developmental lead exposure in the rat. *J. Toxicol. Environ. Health Part A* **1998**, *Part A*, *54*, 101-120, <https://doi.org/10.1080/009841098158944>.
56. Yiin, S.; & Lin, T. Lead-catalyzed peroxidation of essential unsaturated fatty acid. *Biol. Trace Elem. Res.* **1995**, *50*, 167-172, <https://doi.org/10.1007/bf02789419>.
57. Bokara, K.; Brown, E.; McCormick, R.; Yallapragada, P.; Rajanna, S.; & Bettaiya, R. Lead-induced increase in antioxidant enzymes and lipid peroxidation products in developing rat brain. *Biometals* **2007**, *21*, 9-16, <https://doi.org/10.1007/s10534-007-9088-5>.
58. Adegbesan, B.; & Adenuga, G. Effect of lead exposure on liver lipid peroxidative and antioxidant defense systems of protein-undernourished rats. *Biol. Trace Elem. Res.* **2007**, *116*, 219-225, <https://doi.org/10.1007/bf02685932>.
59. Saxena, G.; & Flora, S. Changes in brain biogenic amines and haem biosynthesis and their response to combined administration of succimers and Centella asiaticain lead poisoned rats. *J. Pharm. Pharmacol.* **2006**, *58*, 547-559, <https://doi.org/10.1211/jpp.58.4.0015>.
60. Shafiq-ur-Rehman, Rehman, S.; Chandra, O.; & Abdulla, M. Evaluation of malondialdehyde as an index of lead damage in rat brain homogenates. *Biometals* **1995**, *8*, 275-279, <https://doi.org/10.1007/bf00141599>.
61. Zhao, Y.; Wang, L.; Shen, H.; Wang, Z.; Wei, Q.; & Chen, F. Association Between δ-Aminolevulinic Acid Dehydratase (ALAD) Polymorphism and Blood Lead Levels: A Meta-regression Analysis. *J. Toxicol. Environ. Health Part A* **2007**, *Part A*, *70*, 1986-1994, <https://doi.org/10.1080/15287390701550946>.
62. Flora, S.; Saxena, G.; & Mehta, A. Reversal of Lead-Induced Neuronal Apoptosis by Chelation Treatment in Rats: Role of Reactive Oxygen Species and Intracellular Ca²⁺. *J Pharmacol Exp Ther* **2007**, *322*, 108-116, <https://doi.org/10.1124/jpet.107.121996>.
63. Brennan, P.; Kendrick, K.; & Keverne, E. Neurotransmitter release in the accessory olfactory bulb during and after the formation of an olfactory memory in mice. *Neuroscience* **1995**, *69*, 1075-1086, [https://doi.org/10.1016/0306-4522\(95\)00309-7](https://doi.org/10.1016/0306-4522(95)00309-7).

64. Moreira, E.; Vassilieff, I.; & Vassilieff, V. Developmental lead exposure: behavioral alterations in the short and long term. *Neurotoxicol Teratol.* **2001**, *23*, 489-495. [https://doi.org/10.1016/s0892-0362\(01\)00159-3](https://doi.org/10.1016/s0892-0362(01)00159-3).
65. Hsu, J. Lead Toxicity as Related to Glutathione Metabolism. *J Nutr* **1981**, *111*, 26-33, <https://doi.org/10.1093/jn/111.1.26>.
66. Ito, Y.; Niiya, Y.; Kurita, H.; Shima, S.; & Sarai, S. Serum lipid peroxide level and blood superoxide dismutase activity in workers with occupational exposure to lead. *Int Arch Occup Environ Health* **1985**, *56*, 119-127, <https://doi.org/10.1007/bf00379383>.
67. Sugawara, E.; Nakamura, K.; Miyake, T.; Fukumura, A.; & Seki, Y. Lipid peroxidation and concentration of glutathione in erythrocytes from workers exposed to lead. *Occup. Environ. Med.* **1991**, *48*, 239-242, <https://doi.org/10.1136/oem.48.4.239>.
68. Chiba, M.; Shinohara, A.; Matsushita, K.; Watanabe, H.; & Inaba, Y. Indices of Lead-Exposure in Blood and Urine of Lead-Exposed Workers and Concentrations of Major and Trace Elements and Activities of SOD, GSH-Px and Catalase in Their Blood. *Tohoku J. Exp. Med.* **1996**, *178*, 49-62, <https://doi.org/10.1620/tjem.178.49>.
69. Bhargavi *et al.* A review on detection of heavy metal ions in water – An electrochemical approach. *Sens. Actuators B Chem.* **2015**, *213*, 515-533, <https://doi.org/10.1016/j.snb.2015.02.122>.
70. Tao, Z.; Zhou, Y.; Duan, N.; & Wang, Z. A Colorimetric Aptamer Sensor Based on the Enhanced Peroxidase Activity of Functionalized Graphene/Fe₃O₄-AuNPs for Detection of Lead ²⁺ Ions. *Catalysts* **2020**, *10*, 600, <https://doi.org/10.3390/catal10060600>.
71. Wang, L.; Peng, X.; Fu, H. An Electrochemical Aptasensor for the Sensitive Detection of Pb²⁺ Based on a Chitosan/Reduced Graphene Oxide/Titanium Dioxide. *Microchem. J.* **2022**, *174*, 106977. <https://doi.org/10.1016/j.microc.2021.106977>.
72. Xu, W.; Zhao, A.; Zuo, F.; Khan, R.; Hussain, H.; & Li, J. A highly sensitive DNAzyme-based SERS biosensor for quantitative detection of lead ions in human serum. *Anal. Bioanal. Chem.* **2020**, *412*, 4565-4574, <https://doi.org/10.1007/s00216-020-02709-2>.
73. Wu, W.; Jia, M.; Wang, Z.; Zhang, W.; Zhang, Q.; & Liu, G. *et al.* Simultaneous voltammetric determination of cadmium²⁺, lead²⁺, mercury²⁺, zinc²⁺, and copper²⁺ using a glassy carbon electrode modified with magnetite (Fe₃O₄) nanoparticles and fluorinated multiwalled carbon nanotubes. *Mikrochim Acta* **2019**, *186*. <https://doi.org/10.1007/s00604-018-3216-5>.
74. Wang, Y.; Zhao, G.; Zhang, Q.; Wang, H.; Zhang, Y.; & Cao, W. *et al.* Electrochemical aptasensor based on gold modified graphene nanocomposite with different morphologies for ultrasensitive detection of Pb²⁺. *Sens. Actuators B Chem.* **2019**, *288*, 325-331, <https://doi.org/10.1016/j.snb.2019.03.010>.
75. Wang, N.; Zhao, W.; Shen, Z.; Sun, S.; Dai, H.; Ma, H.; & Lin, M. Sensitive and selective detection of Pb²⁺ and Cu²⁺ using a metal-organic framework/polypyrrole nanocomposite functionalized electrode. *Sens. Actuators B Chem.* **2020**, *304*, 127286, <https://doi.org/10.1016/j.snb.2019.127286>.
76. Wang, L.; Lei, T.; Ren, Z.; Jiang, X.; Yang, X.; Bai, H.; & Wang, S. Fe₃O₄@PDA@MnO₂ core-shell nanocomposites for sensitive electrochemical detection of trace Pb²⁺ in water. *J. Electroanal. Chem.* **2020**, *864*, 114065, <https://doi.org/10.1016/j.jelechem.2020.114065>.
77. Chen, M.; Hassan, M.; Li, H.; & Chen, Q. Fluorometric determination of lead ²⁺ by using aptamer-functionalized upconversion nanoparticles and magnetite-modified gold nanoparticles. *Mikrochim Acta* **2020**, *187*, <https://doi.org/10.1007/s00604-019-4030-4>.
78. Chu *et al.* Visual detection of lead ions based on nanoparticle-amplified magnetophoresis and Mie scattering. *Sens. Actuators B Chem.* **2020**, *306*, 127564, <https://doi.org/10.1016/j.snb.2019.127564>.
79. Khan, M.; Meena, S.; Alam, M.; & Ghosh, S. A solvent sensitive coumarin derivative coupled with gold nanoparticles as selective fluorescent sensor for Pb²⁺ ions in real samples. *Spectrochim. Acta A Mol. Biomol. Spectrosc.* **2020**, *243*, 118810, <https://doi.org/10.1016/j.saa.2020.118810>.
80. Qin, X. An Electrochemical Sensor for Simultaneous Stripping Determination of Cd²⁺ and Pb²⁺ Based on Gold Nanoparticles Functionalized β-cyclodextrin-graphene Hybrids. *Int. J. Electrochem. Sci.* **2020**, 1517-1528, <https://doi.org/10.20964/2020.02.59>.
81. Azimi, H.; Ahmadi, S.; Manafi, M.; Mousavi, S.; & Najaf, M. Development of an analytical method for the determination of lead based on local surface plasmon resonance of silver nanoparticles. *Quim. Nova* **2020**, <https://doi.org/10.21577/0100-4042.20170532>.
82. Yin, H.; Zheng, Y.; & Wang, L. Electrochemical Sensor for Determination of Pb²⁺ Based on Gold Nanoparticles. *J. Nanosci. Nanotechnol.* **2020**, *20*, 3356-3360, <https://doi.org/10.1166/jnn.2020.17415>.

83. Ahmadian-Fard-Fini, S.; Ghanbari, D.; Amiri, O.; & Salavati-Niasari, M. Electro-spinning of cellulose acetate nano-fibers/Fe/carbon dot as photoluminescence sensor for mercury $^{2+}$ and lead $^{2+}$ ions. *Carbohydr. Polym.* **2020**, *229*, 115428, <https://doi.org/10.1016/j.carbpol.2019.115428>.
84. Silva-De Hoyos, L.; Sánchez-Mendieta, V.; Camacho-López, M.; Trujillo-Reyes, J.; & Vilchis-Nestor, A. Plasmonic and fluorescent sensors of metal ions in water based on biogenic gold nanoparticles. *Arab. J. Chem.* **2020**, *13*, 1975-1985, <https://doi.org/10.1016/j.arabjc.2018.02.016>.
85. Dutta, S.; Strack, G.; & Kurup, P. Gold nanostar electrodes for heavy metal detection. *Sens. Actuators B Chem.* **2019**, *281*, 383-39., <https://doi.org/10.1016/j.snb.2018.10.111>.
86. Xu, T.; Dai, H.; & Jin, Y. Electrochemical sensing of lead $^{2+}$ by differential pulse voltammetry using conductive polypyrrole nanoparticles. *Mikrochim Acta* **2019**, *187*, <https://doi.org/10.1007/s00604-019-4027-z>.
87. Zhang, T.; Jin, H.; Fang, Y.; Guan, J.; Ma, S.; & Pan, Y. Detection of trace Cd $^{2+}$, Pb $^{2+}$ and Cu $^{2+}$ ions via porous activated carbon supported palladium nanoparticles modified electrodes using SWASV. *Mater. Chem. Phys.* **2019**, *225*, 433-442, <https://doi.org/10.1016/j.matchemphys.2019.01.010>.
88. Sengan, M.; Kamlekar, R.; & Veerappan, A. Highly selective rapid colorimetric sensing of Pb $^{2+}$ ion in water samples and paint based on metal induced aggregation of N-decanoyltromethamine capped gold nanoparticles. *Spectrochim. Acta A Mol. Biomol. Spectrosc.* **2020**, *239*, 118485, <https://doi.org/10.1016/j.saa.2020.118485>.
89. Silva, C.; Silva, R.; de Figueiredo, A.; & Alves, V. Magnetic Solid-Phase Microextraction for Lead Detection in Aqueous Samples Using Magnetite Nanoparticles. *J. Braz. Chem. Soc.* **2020**, <https://doi.org/10.21577/0103-5053.20190134>.
90. Ryavanaki, L.; Tsai, H.; & Fuh, C. Microwave Synthesis of Gold Nanoclusters with Garlic Extract Modifications for the Simple and Sensitive Detection of Lead Ions. *Nanomaterials* **2020**, *10*, 94, <https://doi.org/10.3390/nano10010094>.
91. Sahu, S.; Sharma, S.; & Ghosh, K. Novel formation of Au/Ag bimetallic nanoparticles from a mixture of monometallic nanoparticles and their application for the rapid detection of lead in onion samples. *New J. Chem.* **2020**, <https://doi.org/10.1039/d0nj02994g>.
92. Kou, Y.; Zhao, Q.; Wang, X.; & Liu, Y. Rapid colorimetric detection of Pb $^{2+}$ with β -cyclodextrin-functionalized nanocrystalline gold. *Mater. Chem. Phys.* **2020**, *243*, 122168, <https://doi.org/10.1016/j.matchemphys.2019.122168>.
93. Venkateswarlu, S.; Reddy, A.; Panda, A.; Sarkar, D.; Son, Y.; & Yoon, M. Reversible Fluorescence Switching of Metal–Organic Framework Nanoparticles for Use as Security Ink and Detection of Pb $^{2+}$ Ions in Aqueous Media. *ACS Appl. Nano Mater.* **2020**, *3*, 3684-3692, <https://doi.org/10.1021/acsnm.0c00392>.